Journal of the Korean Physical Society, Vol. 77, No. 3, August 2020, pp. 247∼252

Formation Mechanism of GaN Nanowires with Various Shapes on Si(111)

Siyun Noh, Sangmoon Han, Ilgyu Choi and Jin Soo Kim*

Department of Electronic and Information Materials Engineering, Division of Advanced Materials Engineering, and Research Center of Advanced Materials Development, Jeonbuk National University, Jeonju 54896, Korea

Mee-Yi Ryu

Department of Physics, Kangwon National University, Chuncheon 24341, Korea

(Received 19 May 2020; revised 3 June 2020; accepted 3 June 2020)

We discuss the formation mechanism of GaN nanowires (NWs) with various shapes grown on Si(111) by using a plasma-assisted molecular-beam epitaxy. The GaN NWs have not only symmetrical structures but also various features such as reverse-mesa and reverse-funnel shapes. To manipulate the shape of GaN NWs, we controlled the growth kinetics of gallium (Ga) atoms by varying V/III ratio, defined as the ratio of the nitrogen (N) flux to the Ga flux, and the growth time. Narrow linewidth broadenings of the x-ray diffraction rocking curves and the coherent crystal structure, which are confirmed by using Cs-corrected transmission electron microscope images, indicate the formation of highly crystalline GaN NWs. The formation of GaN NWs, particularly reverse-funnel shaped NWs (RFS-NWs), can be explained by using the *so-called* wedding-cake growth mechanism, which is related to a reduction in the number of Ga atoms reaching the top surfaces of the GaN NWs from the surface of SiN_x/Si(111) as the height of the GaN NWs increases. Photoluminescence spectra from the GaN RFS-NWs show a double-peak feature at wavelengths of 361.79 and 373.58 nm, which is attributed to two different widths of the GaN NWs in the vertical direction.

Keywords: GaN, Nanowire, Si, Growth mechanism
DOI: 10.3938/jkps.77.247

I. INTRODUCTION

In these days, III-nitride semiconductor materials are being actively studied for applications in optoelectronic devices, such as a light-emitting diode and a photodetector, covering the wavelength window from deep ultraviolet to near infrared by controlling the composition of (Ga, In, Al)N [1]. Particularly, III-nitride nanostructures have advantages in terms of improvement device performances, including improved quantum efficiency and reduced influence of external temperature. Recently, III-nitride nanowires (NWs) have been studied in terms of fundamental physics and potential device applications due to their outstanding electrical and optical properties [2]. According to previous reports, III-nitride NWs are typically grown by using a vapor-liquid-solid (VLS) process, metal organic vapor phase epitaxy, and hydride vapor phase epitaxy [3]. In particular, the VLS process using metal catalysts as initial nucleation sites has been largely used for the growth of GaN NWs [4]. However, forming GaN NWs with high-crystal quality is difficult because of the diffusion of metal catalysts into NWs, which can result in chemical contamination [5,6]. As an example, Au and Ni are typically used as catalytic metals for the VLS growth of GaN NWs. However, they introduce deep-trap levels in the semiconductor band-gap due to the chemical contamination, limiting the performances of optoelectronic devices [6]. If this kind of unexpected effect caused by the metallic catalysts is to be reduced, no catalyst or a self-catalyst is used in the VLS process or the Volmer-Weber mode to form GaN NWs on Si(111) [7,8]. However, forming highly crystalline GaN NWs is still difficult because of the large difference in material parameters including the lattice constants and the thermal expansion coefficients, between GaN and Si. To overcome this problem, S. Han *et al.* used gallium (Ga) droplets, created by using a Ga pre-deposition method, for the growth of GaN NWs on Si(111) [9]. Because Ga droplets can act as self-catalysts, the chemical contamination in GaN NWs is expected to be significantly reduced [10]. In addition, the structural and the optical properties of GaN NWs can be manipulated by controlling the growth conditions for the Ga droplets and subsequent NWs. Compared to epitaxial films, a NW system has important advantages in that the NWs can be separated from the substrate and applied to fabricate

*E-mail: kjinsoo@jbnu.ac.kr

various devices with foreign materials [11]. If the advantages of GaN NWs are to be used, GaN NWs with high crystal quality must be formed. Form this point of view, the formation mechanism of GaN NWs without defects and dislocations needs to be understand in detail.

In this paper, we discuss the growth mechanism of GaN NWs with various shapes on Si(111). The shape of GaN NWs was changed by the controlling growth behavior of the Ga atoms by varying the V/III ratio, which is defined as the ratio of the nitrogen (N) flux to the Ga flux, and the growth time. Particularly, we report the growth behavior of reverse funnel-shaped GaN NWs (GaN RFS-NWs). The formation mechanism of GaN RFS-NWs is explained by using the *so-called* wedding-cake growth mechanism, which is largely related to the number of Ga atoms on the top surfaces of GaN the NWs.

II. EXPERIMENTS

GaN NWs were grown on n-type Si(111) substrates by using plasma-assisted molecular-beam epitaxy (MBE). The native oxide on the Si(111) substrate was removed by using an *in-situ* annealing process at a substrate temperature of 900 °C. Before the growth of the GaN NWs, only a N-plasma flux was supplied to the Si(111) substrate for 10 minutes at 800 °C (nitridation process) to form a SiN_x layer with a thickness of 27 nm. After the nitridation process, only a Ga flux was supplied to the SiN_x/Si(111) substrate to form Ga droplets for the subsequent growth of GaN NWs, which is the Ga pre-deposition method [9,10]. The size and the spatial density of the Ga droplets working as nucleation sites for the formation of GaN NWs were determined by using the supply time of the Ga flux. After the Ga pre-deposition process, Ga and N-plasma fluxes were simultaneously supplied to form of GaN NWs via Ga droplets. To form GaN NWs with high crystal quality, we varied the V/III ratio and the growth time. GaN NWs were grown using V/III ratios of 193 (NW1), 258 (NW2), 322 (NW3), and 471 (NW4) for 4 hours. The V/III ratio was varied by changing the N-plasma flux at a fixed Ga flux of 4.6×10^{-8} Torr. The growth time for the GaN NWs were 2 (NW5), 4 (NW2), and 6 hours (NW6) at a fixed V/III ratio of 258. The details of the growth conditions for GaN NWs are presented in Table 1.

The structural properties of the GaN NWs were analyzed by using field emission-scanning electron microscopy (FE-SEM, HITACHI SU-70), double-crystal X-ray diffraction (DCXRD, RIGAKU MAX-2500), and Cs-corrected transmission electron microscopy (Cs-TEM, JEOL JEM-ARM200F). Photoluminescence (PL) spectroscopy was used to investigate the optical properties of the GaN RFS-NWs, where a diode-pumped solid-state laser with a wavelength of 266 nm and a charge-coupled device with an electrically controlled cooling system were used as the excitation source and the detector, respectively.

Table 1. Growth conditions for GaN NWs.

Sample	V/III ratio (Arb. Units)	Growth time (hour)
NW1	193	4
NW2	258	4
NW3	322	4
NW4	471	4
NW5	258	2
NW6	258	6

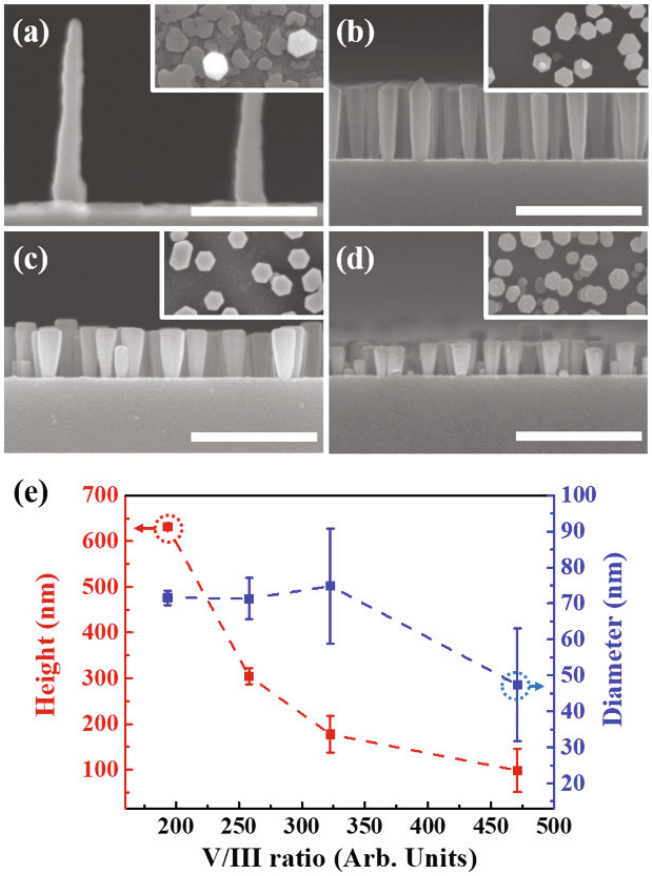

Fig. 1. Cross-sectional FE-SEM images of (a) NW1, (b) NW2, (c) NW3, and (d) NW4 samples grown under different V/III ratios, where the inset shows the plan-view image. The scale bars correspond to 500 nm. (e) Average height and diameter of GaN NWs as functions of the V/III ratio.

III. RESULT AND DISCUSSION

Figure 1 shows cross-sectional FE-SEM images for the (a) NW1, (b) NW2, (c) NW3, and (d) NW4 samples. The inset of each FE-SEM image is a plan-view image

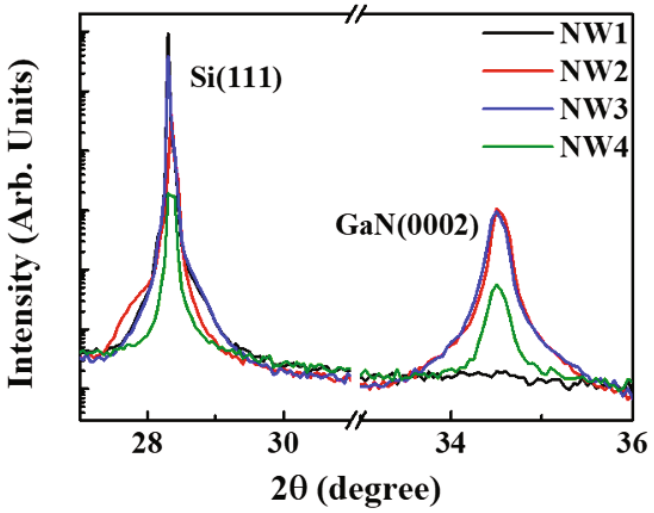

Fig. 2. DCXRD rocking curves for the GaN NWs grown using different V/III ratios for 4 hours.

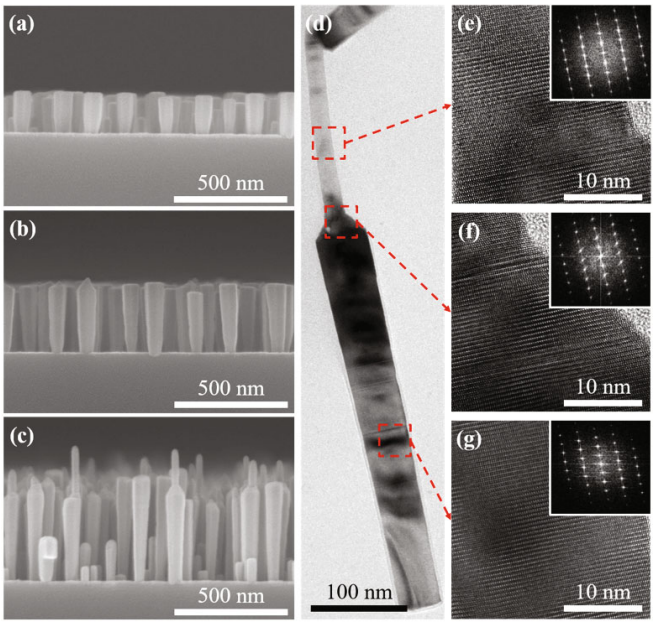

Fig. 3. Cross-sectional FE-SEM images for (a) NW5, (b) NW2, and (c) NW6 samples. (d) Cs-TEM and HR-TEM images for the (e) top, (f) middle, and (g) bottom regions of a GaN RFS-NW. The insets show SAED patterns.

of the GaN NWs. The FE-SEM images clearly show a change in the shape and the structural dimension of the GaN NWs, depending on the V/III ratio. At a V/III ratio of 193, longer GaN NWs with symmetric shapes were formed compared to those grown at a relatively high V/III ratio. GaN NWs were toward a reverse-mesa shape with increasing V/III ratio. This is attributed to the blocking effect of the N atom, which obstructs the migration of Ga atoms upward from the SiN_x/Si(111) substrate [12,13]. Two possible components of Ga atoms contribute to the growth of GaN NWs. One is the Ga atoms directly impinging on the top surfaces of the GaN NWs, and the other is components that first reach the SiN_x/Si(111) substrate and then migrate to the top surface through the sidewalls of the GaN NWs [14,15]. However, the migration of Ga atoms toward the top surfaces of the GaN NWs via the sidewalls is limited by the N atoms in the MBE chamber. This blocking effect of N atoms changes the shape and the height of the GaN NWs. The average heights (diameters) of the NW1, NW2, NW3, and NW4 samples were 631.2 (71.5), 304.6 (71.3), 177.5 (74.8), and 98.3 nm (47.4 nm), respectively. The average heights and diameters of GaN NWs are summarized in Fig. 1(e). With increasing in the V/III ratio, the spatial density of GaN NWs is increased, which is clear when considering the FE-SEM images in the insets. This can be also explained by N atoms blocking the migration of Ga atoms. The migration of Ga atoms via the sidewalls toward the top surfaces of the GaN NWs can be restricted under a high N-rich condition. As a result, Ga atoms, which are unable to migrate toward the top surfaces of the GaN NWs, generate additional nucleation sites on the SiN_x/Si(111) substrate to form additional GaN NWs. Interestingly, conical features are additionally observed on the top surfaces of the GaN NWs, as shown in Fig. 1(b), which will be discussed at Fig. 3.

Figure 2 shows DCXRD rocking curves for the NW1, NW2, NW3, and NW4 samples. The DCXRD peaks are in good agreement with GaN in the wurtzite (WZ) structure and Si with the cubic structure [16]. The strong peak at 28.32° corresponds to Si(111), where the asymmetric Gaussian feature is attributed to the difference in material parameters between SiN_x and Si(111). The peak related to GaN(0002) is clearly observed at 34.5° for the NW2, NW3, and NW4 samples. In case of the NW1 sample, the peak corresponding to GaN(0002) was not observed because of the low spatial density of GaN NWs, as shown in Fig. 1(a). For the NW2, NW3, and NW4 samples, the peak positions corresponding to GaN(0002) are slightly shifted with increasing average height of GaN NWs. This is attributed to a reduced tensile strain caused by the large difference in material parameters between GaN and Si(111) [17]. That is, the tensile strain between GaN and Si(111) diminishes as the height of the GaN NWs increases. The peak intensity of GaN(0002) for the NW3 sample is similar to that for the NW2 sample. This result is related to the volumes of GaN NWs being similar due an increase in the width. For the NW4 sample, the peak GaN(0002) intensity is drastically reduced compared to that for the NW3 sample. This is related to the influence of the stacking faults formed at the interface between GaN and SiN_x/Si(111), which are typically observed in Si-based III-V semiconductor NWs. The GaN(0002) peaks have narrow full widths at half maximum (FWHMs) of 0.17, 0.17, and 0.19° for the NW2, NW3, and NW4 samples, respectively. These FWHMs are relatively narrow compared

to those (∼1.3°) in previous works [18, 19], indicating the formation of highly crystalline GaN NWs with an effective WZ structure on Si(111).

In the FE-SEM image of Fig. 1(b), additional features can be observed on the top surfaces of the GaN NWs. To analyze this structure more deeply, we varied the growth time for the GaN NWs. Figures 3(a), 3(b), and 3(c) show cross-sectional FE-SEM images of the NW5 (2 hours), NW2 (4 hours), and NW6 (6 hours) samples, respectively. The average height of the GaN NWs for the NW5 sample was 179.6 nm. As clearly shown in the FE-SEM images, the height of the GaN NWs increased as the growth time was increased. For the NW2 sample, conical features were additionally observed on the top surfaces of the GaN NWs, which are clearly different from the shape of the NW5 sample, when the height of the NWs reached 350 nm or more. With further increasing growth time, a relatively thin GaN NW was formed on the top surface of thick one. Namely, GaN RFS-NWs were formed. Figure 3(d) shows the Cs-TEM image of the GaN RFS-NW with two different widths along the vertical direction. The lengths (diameters) of the bottom thick and the top thin parts were measured as 394.8 (46.4) and 202.6 (18.8) nm, respectively. In the interfacial region, the thickness changed gradually. Figures 3(e), 3(f), and 3(g) show high-resolution (HR) TEM images measured at the top, middle, and bottom regions of the GaN RFS-NW, respectively. Stacking faults and defects are rarely observed in all HR-TEM images. The inset of each image shows the selective area electron diffraction (SAED) pattern. The SAED patterns for all the regions of the GaN RFS-NWs represent the WZ structure, indicating the formation of GaN NWs with high crystal quality. This result is consistent with the DCXRD results shown in Fig. 2.

According to previous reports, the role of screw dislocations is significant for the growth of NWs [20,21]. That is, the growth process of GaN NWs can be explained by using the screw dislocation-driven mechanism. However, dislocations were not observed vertically along the growth direction in the position-dependent TEM images of our GaN NWs. Therefore, the growth process of the GaN NWs in this work did not depend on the screw dislocation-driven growth mechanism. To explain the growth mechanism of GaN RFS-NWs, we considered an appropriate growth model, a wedding-cake growth mechanism. X. Yin *et al.* invoked the wedding-cake growth mechanism to explain the formation of NWs with defect-free crystals [22], where the formation of the nanostructure was related to an increase in the diffusion length of adatoms as the supply rate of atoms was decreased. In the wedding-cake growth model, we consider that the growth of GaN NWs proceeds only under a homogeneous condition, where no foreign atoms, except Ga and N, are involved in the nucleation and additional growth. Figure 4 shows a schematic illustration for the formation of GaN RFS-NWs. As mentioned above, Ga atoms supplied from an effusion cell reach both the SiN_x/Si(111) substrate and the top surfaces of the GaN NWs. Ga adatoms reaching SiN_x/Si(111) directly receive thermal energy from the substrate, resulting in diffusion through the sidewalls toward the top surfaces of the GaN NWs. The migration length of Ga atoms, however, is limited due to the fixed growth temperature. The formation of GaN NWs with a slight reverse-mesa structure is related to the limited migration length of Ga atoms under a N-rich condition. That is, Ga atoms traveling through the sidewalls to the top surfaces of GaN NWs cannot migrate beyond a certain distance; consequently, the number of Ga atoms reaching the top surfaces of the GaN NWs is dramatically reduced. In the modified wedding-cake growth mechanism, the lateral growth rate of the GaN NWs is proportional to the number of Ga atoms at a fixed N-flux. Above a certain height of GaN NWs, as a result, the lateral growth of the GaN NWs is significantly reduced. On the other hand, the additional nucleation of GaN NWs caused by Ga atoms directly reaching on the top surfaces is dominant. In addition, Ga atoms reaching the top surfaces of the GaN NWs from the effusion cell cannot overcome the energy barrier at the step edge, called the Ehrlich-Schwoebel (ES) barrier, to diffuse down to the vertical facets [23, 24]. Thus, the lateral growth of GaN NWs is restricted at the step edge. The vertical growth rate of GaN NWs is inversely proportional to the critical size of the top terrace [25]. Because GaN NWs have narrow effective areas on the top surfaces, the possibility for the formation of GaN NWs along the vertical direction via additional nucleation site is increased. As a result, GaN RFS-NWs with two different widths were formed, as shown in the FE-SEM image for the NW6 sample.

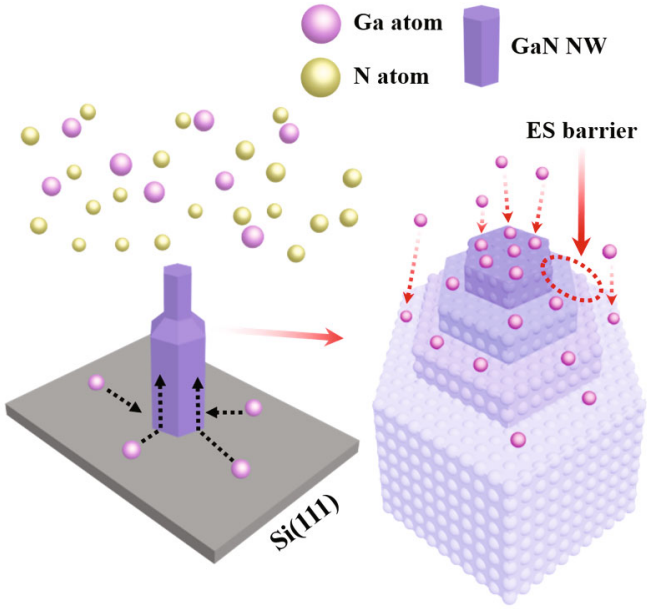

Fig. 4. Schematic illustration for the formation of a GaN RFS-NW.

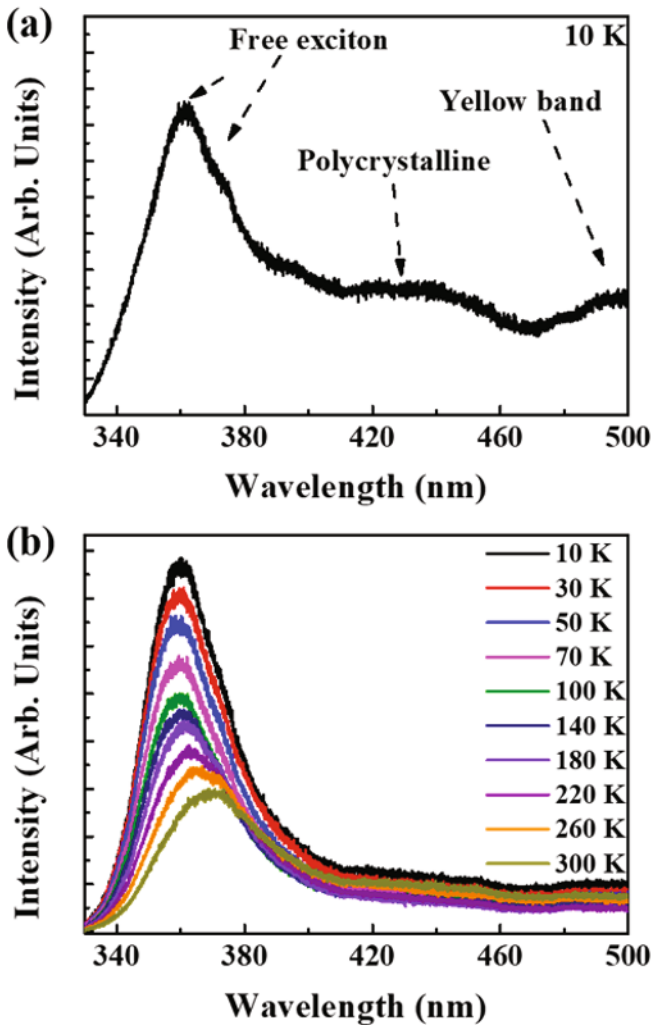

Fig. 5. PL spectra of GaN RFS-NWs measured at temperatures ranging from 10 to 300 K.

Figure 5 shows PL spectra for GaN RFS-NWs measured at temperatures ranging from 10 to 300 K, where the excitation intensity was 20 mW/cm^2. In previous reports, the PL peak of the GaN NWs was observed at a wavelength around 360 nm at low temperatures (10 K) [26,27]. Because Si-based III-nitride NWs typically contain defects, including stacking faults, mostly caused by the use of a foreign substrate, measuring the free exciton (FX) peaks at room temperature is not easy. That is, photo-excited carriers can be trapped at the structural defects of the nanostructures, typically resulting in their non-radiative recombination [28]. For GaN RFS-NWs in this study, however, two strong FX peaks were clearly observed at room temperature. Once again, this result indicates the formation of highly crystalline GaN NWs. At 10 K, the FX peaks were measured as 362 and 374 nm. The double FX peaks are related to two different widths of GaN NWs in the vertical direction. That is, the thickness difference between the top thin and the bottom thick parts of the GaN NWs results in a change in quantum size effect [29]. Figure 5(b) shows the temperature dependence of the PL spectra for the GaN RFS-NWs. The PL spectrum is red-shifted from 362 to 370 nm with increasing temperature. This shift results from the enhanced electron-phonon interaction with increasing temperature [30]. The FWHMs of the PL spectra varied from 26 to 34 nm as the temperature was increased, which is also attributed to the enhanced electron-phonon coupling.

IV. CONCLUSION

In summary, we discussed the formation mechanism of GaN NWs having various shapes on SiN_x/Si(111). According to the FE-SEM, DCXRD, and Cs-TEM results, highly crystalline GaN NWs were formed. The formation of GaN NWs with various shapes grown under different V/III ratio conditions was related to the growth behavior of Ga atoms directly influenced by N atoms. Due to the drastic change in the number of Ga atoms on the top surfaces of the GaN NWs, GaN RFS-NWs with two different widths along the vertical direction were formed. To explicate the formation of GaN RFS-NWs, we used the wedding-cake growth mechanism, which is a suitable model for explaining the growth of defect-free crystalline NWs. The PL spectra from the GaN RFS-NWs showed a double-peak feature, which could be attributed to the quantum size effect in the vertical direction of the NWs.

ACKNOWLEDGMENTS

The work was supported in part by the National Research Foundation of Korea (NRF) funded by the Ministry of Education (2018R1D1A1B07043442), by the Civil-Military Technology Cooperation Program (No. 19-CM-BD-05), and by the "Research Base Construction Fund Support Program" funded by Jeonbuk (Chonbuk) National University in 2018.

REFERENCES

[1] C. S. Kim *et al.*, J. Korean Phys. Soc. **57**, 793 (2010).
[2] S. Han *et al.*, J. Electron. Mater. **47**, 944 (2018).
[3] G. Avit *et al.*, Nano Lett. **14**, 559 (2014).
[4] C. B. Maliakkal *et al.*, Nano Lett. **16**, 7632 (2016).
[5] D. W. Park *et al.*, Sci. Rep. **5**, 16652 (2015).
[6] Y. Wang, V. Schmidt, S. Senz and U. Gösele, Nanotechnology **1**, 186 (2006).
[7] S. Eftychis *et al.*, J. Cryst. Growth **442**, 8 (2016).
[8] S. Fernández-Garrido *et al.*, Nano Lett. **13**, 3274 (2013).
[9] S. Han *et al.*, ACS Appl. Mater. Interfaces **10**, 38173 (2018).
[10] I. Choi *et al.*, Nanotechnology **29**, 315603 (2018).

[11] C. Zhao *et al.*, Prog. Quantum Electron. **61**, 1 (2018).
[12] V. Consonni, A. Trampert, L. Geelhaar and H. Riechert, Appl. Phys. Lett. **99**, 033102 (2011).
[13] F. Gao *et al.*, Small **13**, 1603775 (2017).
[14] R. K. Debnath *et al.*, Appl. Phys. Lett. **90**, 123117 (2007).
[15] K. A. Bertness *et al.*, J. Electron. Mater. **35**, 576 (2006).
[16] G. Santana *et al.*, Materials **6**, 1050 (2013).
[17] V. M. Kaganer *et al.*, J. Phys. D: Appl. Phys. **48**, 385105 (2015).
[18] V. P. Kladko *et al.*, J. Cryst. Growth **401**, 347 (2014).
[19] S. Eftychis *et al.*, J. Cryst. Growth **514**, 89 (2019).
[20] F. Meng, S. A. Morin, A. Forticaux and S. Jin, Acc. Chem. Res. **46**, 1616 (2013).
[21] M. J. Bierman *et al.*, Science **320**, 1060 (2008).
[22] X. Yin *et al.*, Nano Lett. **15**, 7766 (2015).
[23] G. Ehrlich and F. G. Hudda, J. Chem. Phys. **44**, 1039 (1966).
[24] R. L. Schwoebel and E. J. Shipsey, J. Appl. Phys. **37**, 3682 (1966).
[25] J. Krug, Physica A 313, 47 (2002).
[26] C. H. Wu *et al.*, J. Cryst. Growth **454**, 71 (2016).
[27] L. W. Tu, C. L. Hsiao, T. W. Chi and I. Lo, Appl. Phys. Lett. **82**, 1601 (2003).
[28] Y. H. Ra, R. Navamathavan, J. H. Park and C. R. Lee, Nano Lett. **13**, 3506 (2013).
[29] D. Kandi, S. Martha and K. M. Parida, Int. J. Hydrog. Energy **42**, 9467 (2017).
[30] K. O'Donnell and X. Chen, Appl. Phys. Lett. **58**, 2924 (1991).